Structural and electronic properties of graphite via an all-electron total-energy local-density approach

H. J. F. Jansen
Department of Physics, Northwestern University, Evanston, Illinois 60201
and Department of Physics, Oregon State University, Corvallis, Oregon 97331

A. J. Freeman
Department of Physics and Astronomy, Northwestern University, Evanston, Illinois 60201
(Received 31 October 1986)

The electronic and structural properties of graphite have been determined in the local-density approximation with our precise total-energy full-potential linearized augmented-plane-wave method. We confirm the presence of a low-lying unoccupied Γ_1^+ interlayer state, which is of importance for intercalation compounds. A careful study of the convergence of the numerical results was needed in order to obtain reliable data for the total energy. Our values of the lattice parameters and their pressure dependence are in good agreement with experiment. The values of the elastic constants $C_{11}+C_{12}$ and C_{33} agree with their experimental counterparts. The experimental value of C_{13} differs from our result, and is also inconsistent with the experimental results for the lattice parameters under pressure; new experiments are suggested to resolve this inconsistency.

I. INTRODUCTION

Even today, the electronic structure of graphite presents a challenge for solid-state theory because of the presence of two distinct and completely different types of interatomic bonding. Many calculations have been devoted to this material. The differences between the results demonstrate the importance of the numerical approximations made in most of these studies, which focused only on the electronic band structure of graphite.[1-3] Reliable calculations pertaining to structural properties derived from a knowledge of the total energy have only been possible in the last few years;[4,5] their results also show the effects of the numerical problems related to the open atomic structure of graphite.[5]

As previously described, our full-potential linearized augmented-plane-wave (FLAPW) method,[6] like most modern methods, enables us to study the electronic properties for any structure with full control over the numerical approximations. The numerical noise in the total-energy data in this work is less than 1 mRy. As a consequence, the inaccuracies of the results mainly reflect the effects of the local approximation within density-functional theory on the structural properties of graphite. Additionally, these results will serve as a reference for our work on thin films[7] and graphite intercalated compounds.[8] A further benefit of this study is that a comparison with the results of Yin and Cohen[5] (YC) allow a determination of the effects of the pseudopotential approximation. Finally, we are able to extend the previous results of YC (Ref. 5) and to obtain values for some of the elastic constants and the pressure dependence of the lattice constants.

Following Sec. II, which presents a brief description of the method used, some band-structure results are presented in Sec. III. A total-energy study of the cohesive energy and related properties is given in Sec. IV. Detailed total energy determinations of the a and c lattice constants are presented in Sec. V and their pressure dependence in Sec. VI. Results for the bulk modulus and elastic constants are compared with experiment, and discussed in detail in Sec. VII. Numerical details of the precision of the calculations are given in Appendix A and a careful analysis and derivation of the interpolation of the enthalpy is presented as Appendix B.

II. METHOD

The principles of our all-electron FLAPW method are described in detail elsewhere.[6] Here we focus on one important feature of the method which allows comparisons to be made with the results obtained with the pseudopotential method by YC.[5] Following the traditional APW approach of Slater, space is divided into two regions by constructing (non-overlapping) spheres around each nucleus; we expand quantities such as charge density and potential in spherical harmonics inside these spheres and in plane waves outside these spheres. Since the radial equations are solved numerically inside the spheres, the basis functions contain more information than the plane waves used in the pseudopotential method. In the case of graphite this results in a smaller numerical basis (between 500 and 600 functions) and, compared to the pseudopotential method as applied in YC,[5] the loss of time in constructing our basis functions is compensated by the large gain due to the diagonalization of a smaller matrix. This is opposite to the more familiar situation known in simple metals, where basis sizes are much smaller and the pseudopotential method is much more efficient.

Details pertaining to the numerical convergence of our

results are found in Appendix A. Since energy differences turn out to be small, such a study is very important. Surprisingly, the most sensitive parameter governing the relative convergence of our results for different values of the lattice constants is the number of **k** points inside the irreducible wedge of the first Brillouin zone (IBZ) at which the energy bands are evaluated. For each set of values of the lattice parameters we employed up to 140 independent points in the IBZ in the final self-consistent iterations in order to establish the rate of convergence and to be able to extrapolate to a converged result with a precision better than 1 mRy.

III. BAND STRUCTURE

The energy levels of graphite have been studied and discussed by many authors. We therefore only compare our results in Table I with the most recent theoretical work of Refs. 2 and 3. The data of Holzwarth *et al.*[3] presented in this table are based on the same form of the exchange and correlation potential (Hedin-Lundqvist) as we have used; Tatar and Rabii[2] employed the Slater $X\alpha$ form. In general, the qualitative agreement between the results of these three different calculations is good. We clearly confirm Holzwarth *et al.*'s result for the first unoccupied σ band, whose position was the only major discrepancy between the work in Refs. 2 and 3. The nature of this state, which is very important for the graphite intercalation process, has been discussed previously.[8]

It is, however, clear that for a more quantitative analysis, we cannot compare with Ref. 2, since these results are based on a different form of the exchange and correlation potential. Instead, we focus on the results of Ref. 3. Comparing with their results (cf. the first two columns in Table I), we see a large difference between the eigenvalues at the top of the σ band. We found that the energy levels in this case are very sensitive to the number of **k** points used in the iterations, with errors of about 1 eV for the number of **k** points used in Ref. 3. For all other entries in Table I we confirm a numerical precision of 0.2—0.3 eV for the results of Ref. 3 and find our precision to be 0.1—0.2 eV.

The remaining discrepancy for the states far away from the Fermi level between our results and the pseudopotential results of Ref. 3 is not due to any systematic error in the FLAPW method. In this context, we carefully investigated errors connected to the use of an (l-dependent) energy parameter in the numerical integration of the radial Dirac equation.[6] The energy eigenvalues are precise near the middle of the occupied band (corresponding to the position of the energy parameters pertaining to the self-consistent solution). Near the top and bottom of the band we introduce systematic errors, which compensate each other in the evaluation of the total energy and charge density. We have examined this effect by repeating our band-structure calculations, using the same self-consistent density, for values of the energy parameters ranging from -1 to $+1$ Ry relative to the middle of the occupied band. Changes in the eigenvalues are at most 0.02 eV, much less than our precision of 0.1—0.2 eV.

Two factors are important in making quantitative comparisons between theory and experiment.[9–11] First of all, we use a local-density approximation to the true exchange and correlation potential. Secondly, the measured excitation energies are to be obtained from Dyson's equation, which essentially adds self-energy corrections to the true exchange and correlation potential. In graphite it is *a priori* not clear which of those two effects will be the most important. Therefore graphite is an extremely interesting case to treat with improved, nonlocal approximations to the exchange and correlation potential; this should lead to a better understanding of the effects of the two correlations mentioned above.

IV. TOTAL ENERGY

Comparing the total energy of graphite with its atomic counterpart gives the cohesive energy. It is known, however, that because of multiplet effects the local-density approximation underestimates the total energy of a carbon atom, leading to an overestimate of the cohesive energy by about 1.3 eV/atom.[7] A direct comparison with the total energy of a free monolayer, however, is meaningful and gives the interplanar binding energy. Our experience with other materials indicates that in comparing the converged values of the total energy of the bulk and film FLAPW codes we find a difference of at most 4 mRy per atom, and that the total energy calculated with the bulk pro-

TABLE I. Band energies with respect to the Fermi level at the Γ point of graphite (in eV).

	This work	Ref. 3[a]	Ref. 2	Expt.
Bottom σ band	−19.6	−20.8	−19.5	−20.6[b]
	−19.3	−20.5	−19.2	
Bottom π band	−8.7	−9.1	−8.2	−8.1[b], −8.5[d]
	−6.7	−7.1	−6.5	−7.2[b], −5.7[c], −6.6[d]
Top σ band	−4.6	−3.4	−4.3	−4.6[b], −5.5[d]
	−4.6	−3.3	−4.3	
Unoccupied σ bands	3.8	3.7	7.1	
	8.3	9.0	7.3	
	8.4	9.3	7.3	

[a]Hedin-Lundqvist exchange and correlation.
[b]Reference 9 (angle-resolved photoemission).
[c]Reference 10 (angle-integrated photoemission).
[d]Reference 11 (angle-resolved photoemission).

gram is lower.[12]

By carefully monitoring the total energy as a function of all numerical parameters, we predict a value of -302.592 Ry/cell for the total energy at the theoretical equilibrium configuration of graphite. The fully converged value of the total energy of a free monolayer is[13] -302.551 Ry (4 atoms) and hence the interplanar binding energy, which is the difference between the bulk and monolayer energy, becomes 40 mRy/cell or 10 mRy/atom. Adjusting for the systematic difference in results obtained by using the two FLAPW programs, this value is reduced to at most 6 mRy/atom, which still is much larger than the experimental value of 1.5 ± 0.2 mRy/atom,[14] but comparable to the value of 8 mRy/atom obtained in Ref. 4. Taken at face value this difference between experiment and theory indicates that the local-density approximation is inaccurate in the low-density interstitial region. However, one should also keep in mind that the experimental value is very sensitive to the presence of stacking faults, defects, and impurities.

In addition, we calculated the total energy of graphitic layers in the *AAA* stacking mode; we find a value of -151.292 Ry (2 atoms). This leads to an upper bound on the theoretical value of the *AAA* stacking-fault energy of 2 mRy/atom. The experimental value is 0.24 mRy/atom,[14] which indicates that long-range effects are important and that the proper value of the *AAA* stacking-fault energy should be obtained in a calculation where only one graphitic layer is changed from the *B* to the *A* position.

V. LATTICE CONSTANTS

We have evaluated the total energy of graphite for 13 different combinations of the lattice constants a and c (see Appendix A). The results were fitted to a second-order Taylor expansion and the minimum of this function yielded our values of the lattice constants. These numbers are presented in Table II, together with experimental[15–17] and other theoretical results. The error bars on our theoretical values are partly due to the relative precision of our data, but also due to the fact that in our range of values of a and c third-order terms in the Taylor expansion are not negligible. We do not have enough data to reliably determine the exact values of the third-order derivatives; to do so we should, at least, double the number of calculated data points. We are, however, able to derive realistic estimates for their magnitude when we assume that we can neglect terms of fourth order. In this kind of analysis one uses orthogonal polynomials—in our case Legendre polynomials—mapped onto the ranges of a and c. As a result, these third-order terms do directly change the values of the lattice constants and also indirectly alter the values for the elastic constants at zero pressure because the position of the minimum is changed. For details we refer to Appendix B; here we only remark that we have included the effects of higher order terms in our error estimates.

As is clear from Table II, the theoretical values of the in-plane lattice constant a are in excellent agreement with the experimental numbers. It turns out that the minimum of the total energy is very sharp along lines of constant c, and this leads to a small uncertainty in our theoretical value of a. Apparently, the strong covalent bond between the carbon atoms in a graphitic plane is fairly well described by local-density theory. Also, since there are only two $1s$ core electrons per atom the pseudopotential method should work very well, and it does.[5]

TABLE II. Comparison of theoretical and experimental values of the lattice constants of graphite (in Å).

	a	c
Theory (this work)	2.459 ± 0.006	6.828 ± 0.059
Theory[a] (pseudopotential)	2.47	6.73 (7.05)
Theory[b] (Thomas-Fermi)		5.60
Theory[c] (FLAPW, monolayer)	2.450	
Expt. (room temperature)[d]	2.456	6.696
Expt. (room temperature)[e]	2.4612	6.7078
Expt. (zero temperature)[f]	2.462	6.656

[a]Reference 5, derived with c/a ratio fixed at the experimental value. The second value for c (given in parentheses) is derived from an unconstrained calculation with independent variations of a and c.
[b]Reference 4.
[c]Reference 7.
[d]Reference 15.
[e]Reference 16.
[f]Reference 17.

By contrast, calculated energy differences due to changes along the c axis are much smaller and hence the error bar on our theoretical value is much larger. The difference between our value and the experimental number is about three standard deviations, and we interpret this difference to be due to errors in the local-density approximation. The electronic charge density between the graphitic planes is much smaller than in the planes, and the Hedin-Lundqvist approximation is known to underestimate the potential in such a region of low density. This results in a weaker bonding between the planes and a value of the lattice constant c which is too large. It would be very interesting to see how nonlocal approximations to the exchange and correlation potential affect this result.

Table II also compares our results with those of other theoretical calculations. The pseudopotential method[5] gives a slightly better (i.e., smaller) value for c, but in this case this number is mainly determined by the value of a, since the ratio c/a was kept fixed at the experimental value. Varying c independently of a yielded a much poorer pseudopotential result (7.05 Å), but the authors do not state the size of their numerical error due to an incomplete basis. The very poor result of Ref. 4, derived from a simple Thomas-Fermi model, shows that this approach is too crude to obtain accurate values for the lattice constants, although it is certainly a useful method for comparing the relative effects due to intercalation. Finally, a comparison of our results for bulk graphite with the value of a determined from an earlier thin-film FLAPW calculation for the monolayer[7] shows very good overall agreement. The difference lies outside error bars in the numerical precision of both calculations and reinforces the speculation[7] that the difference between the calculated a

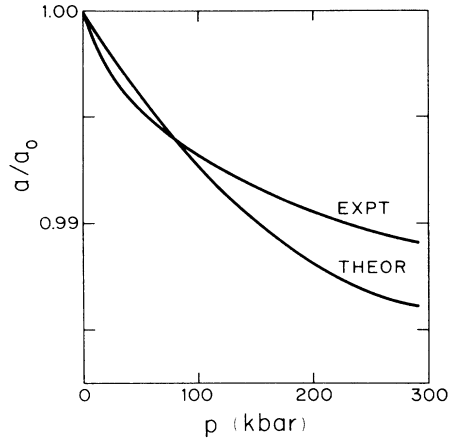

FIG. 1. Experimental (Ref. 16) and theoretical values of the relative change of the lattice constant a with pressure.

value for a monolayer and experiment may reflect a real effect. It appears to be consistent with the observed behavior of the a and c parameters with temperature.

VI. PRESSURE DEPENDENCE OF THE LATTICE CONSTANTS

Given the internal energy of graphite as a function of a and c, one may easily obtain the enthalpy by adding the product of pressure and volume. Minimizing the enthalpy then yields the lattice constants at zero temperature as a function of pressure. Figures 1 and 2 display the experimental[16] and theoretical values of the relative changes in the lattice constants as a function of pressure. Note, however, that the experimental data are taken at room temperature, and that some caution is necessary before making a comparison. Inspection of Table II shows that changes due to cooling to 0 K (Ref. 17) are about 0.2% for a and about 0.6% for c. We can assume, however, that the relative effect of pressure on these corrections is much smaller. This means that the difference between the theoretical and experimental results in Figs. 1 and 2 is

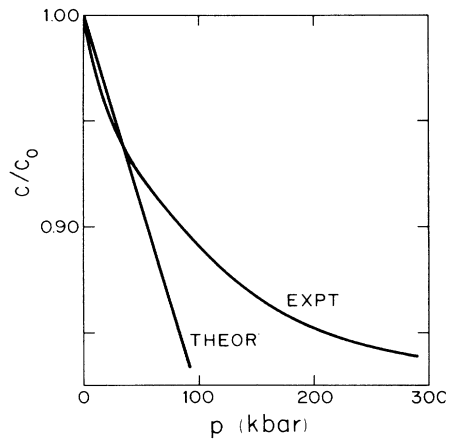

FIG. 2. Experimental (Ref. 16) and theoretical values of the relative change of the lattice constant c with pressure.

TABLE III. Comparison of experimental and theoretical values of the c/a ratio as a function of pressure.

Pressure (kbar)	$(c/a)/(c_0/a_0)$ Experiment (Ref. 16)	Theory (this work)
7.8	0.9839	0.986
17	0.9667	0.970
27	0.9498	0.953
48	0.9329	0.916

probably not due to temperature effects.

We have calculated the total energy of graphite for values of a/a_0 between 0.98 and 1.04 and values of c/c_0 between 0.90 and 1.10 and hence our interpolation is only valid for this region. This immediately explains why we find a large discrepancy for c/c_0 at pressures above 60 kbar; in this case we are outside the range of validity for our interpolation of the enthalpy. Additionally, Figs. 1 and 2 show systematic deviations. They underestimate the changes at low pressure and overestimate the changes at higher pressure. These systematic deviations point to the importance of higher-order terms in the expansion of the enthalpy, which is consistent with what we have found before. For this reason, we expect third-order terms in the Taylor expansion of the total energy to be the main cause of the difference between experiment and theory in Figs. 1 and 2, and we think that the effects of the local-density approximation are much less important.

When we restrict ourselves to pressures less than 50 kbar, we can directly compare the experimental and theoretical values of the c/a ratio under pressure. As seen from the results given in Table III the agreement here is very good; the error is still only 2% at 48 kbar, but then rises strongly with pressure, because our extrapolation for c becomes inaccurate.

The calculated and experimental values of the derivatives of the lattice constants with pressure at zero pressure are presented in Table IV. We see that our calculated values are smaller than the experimental room-temperature values, consistent with Figs. 1 and 2. These pressure derivatives, however, are directly related to the values of the elastic constants, as will be discussed later. The measured temperature dependence of the elastic constants then allows us to derive the derivatives of a and c with pressure at zero temperature (see below). The result-

TABLE IV. Theoretical and experimental values of the derivative of the lattice constants with pressure in Mbar^{-1}, at zero pressure.

	$-\frac{\partial}{\partial p}\left[\frac{a}{a_0}\right]$	$-\frac{\partial}{\partial p}\left[\frac{c}{c_0}\right]$
This work	0.09±0.03	1.82±0.42
Expt.[a] (300 K)	0.18±0.01	2.40±0.05
Expt.[b] (extrapolated to 0 K)	0.20±0.01	2.29±0.05

[a]Reference 16.

[b]Extrapolation to 0 K based on the temperature dependence of the elastic constants as measured in Ref. 19.

TABLE V. Theoretical and experimental values of the bulk modulus, B, and isotropic bulk modulus, B_{iso}, of graphite in Mbar.

	B	B_{iso}
This work	0.50±0.08	3.19±0.21
Expt.[a] (300 K)	0.36±0.01	2.86±0.11
Expt.[b] (0 K)	0.41±0.01	3.18±0.11
Expt.[c] (300 K)	0.36±0.01	

[a]Reference 18, from elastic constants.
[b]Reference 19, from elastic constants.
[c]Reference 16, from lattice constants.

ing values are shown on the third line of Table IV. At this point we emphasize that the difference between theory and experiment for $\partial/\partial p(c/c_0)$ is of the same magnitude as the error in our theoretical value, which incorporates higher-order effects. The difference for $\partial/\partial p(a/a_0)$, however, is much larger. We will see that this value is strongly influenced by errors in C_{13}, and that in this case the extrapolation to zero temperature may possibly be inaccurate.

VII. ELASTIC CONSTANTS

Table V compares theoretical and experimental values of the bulk modulus and the isotropic bulk modulus (obtained from volume changes with constant c/a ratio) for graphite as a function of pressure. The agreement between theory and experiment[16,18,19] at $T=0$ K is especially good for the isotropic bulk modulus. Now, as is well known, both bulk moduli are linear combinations of the elastic constants. As a result of the anisotropic nature of the interactions in graphite the lattice is very stiff only in the graphitic planes, and hence C_{11} is much larger than the other constants. Hence the good agreement found in Table V does not necessarily imply good values for all of the elastic constants separately.

In order to investigate the elastic constants in more detail, we have fitted our total-energy data as a function of a and c to second order. In doing so we have applied uniform distortions only in the graphitic plane, conserving the overall symmetry. We did not attempt to calculate symmetry breaking distortions because this would increase the computing time beyond reasonable limits. As a result we are only able to determine the elastic constants C_{33}, C_{13}, and the combination $C_{11}+C_{12}$ (which can only be separated by deforming the carbon rings). The fifth constant, C_{44}, pertains to shear deformations of the planes which also reduce the symmetry.

Table VI shows our results. As expected, our value of $C_{11}+C_{12}$ agrees well (within our error bar) with experiment at zero temperature (third line in Table VI). The errors in C_{13} and C_{33} are much larger; our negative value of C_{13} is especially surprising (although it is zero within the error bar). Note, however, that the error in C_{13} is consistent with the error in the value of c discussed earlier. One can obtain our theoretical value of c in a hypothetical experiment by applying a negative pressure of about 75 kbar. This would bring down the value of C_{13} by 0.24 Mbar (Ref. 19) and yield a room-temperature value of -0.09 Mbar. Extrapolating this value to 0 K would make C_{13} again positive, but its exact magnitude is uncertain.[19] Such a result, however, is in contradiction with our theoretical values of a, $C_{12}+C_{12}$, and C_{33}, which are all consistent with an experiment in which we apply a positive pressure of about 15 kbar. Hence, it is quite apparent that a proper treatment of the highly anisotropic nature of graphite plays a very important role in determining the elastic constants. As a next step we calculated the values of the pressure derivatives of the lattice constants directly from the elastic constants [see Appendix B, Eq. (B17)]. The value of $(\partial c/\partial p)(2.74\pm0.17$ Mbar^{-1} at 300 K) is about 15% different from the direct experiment; this number is mainly determined by C_{33}. A very large difference, however, is found for $\partial a/\partial p$. The value derived from the elastic constants is 0.05 ± 0.02 Mbar^{-1} at 300 K. At zero temperature, the elastic constants C_{13} and C_{33} are almost equal and this yields an extremely small value for the change in a with pressure (0.00 ± 0.02 Mbar^{-1}). This result clearly contradicts the direct measurement.

We now invert this process. We assume that the experimental value of $C_{11}+C_{12}$ is correct, but use the data on the pressure derivatives of the lattice constants to obtain values for C_{13} and C_{33}. The room-temperature results are shown on the fourth line of Table VI. Since the measurements[19] of the temperature effects were only relative, we can directly use these results to scale the values to zero temperature, and these results are shown on the fifth line of Table VI. (These values were then used to obtain the

TABLE VI. Theoretical and experimental values of the elastic constants of graphite in Mbar. The last two lines show rederived experimental values based on the pressure dependence of the lattice constants, as described in the text.

	$C_{11}+C_{12}$	C_{33}	C_{13}
This work	14.3±1.7	0.56±0.09	−0.12±0.13
Expt.[a] (300 K)	12.4±0.4	0.36±0.01	0.15±0.05
Expt.[b] (0 K)	13.3±0.4	0.41±0.01	0.40±0.05
Rederived experiment (300 K)	12.4±0.4	0.49±0.03	−0.51±0.06
Rederived experiment (0 K)	13.3±0.4	0.56±0.03	−0.71±0.06

[a]Reference 18.
[b]Reference 19.

third line in Table IV, discussed earlier, which gives the pressure derivatives of the lattice constants at zero temperature.) The value for C_{33} obtained in this way is in good agreement with our theoretical value (cf. line one). We see that C_{13} is negative, but again its value is very different from our theoretical value. A negative value of C_{13} is, at first sight, in contradiction with the measured values of the thermal expansion coefficients. An analysis by Kelly[20] shows that this is not true; even with the standard value of C_{13} one needs a large phonon contribution to explain the observed contraction of the a axis with temperature.

We now have to ask why the values of C_{13} shown in Table VI are so different. When C_{13} becomes larger than C_{33}, the a axis will expand with pressure, which is not observed. Hence C_{13} has to be smaller than C_{33}. From Appendix B [Eq. (B17)] we see that for graphite we have approximately

$$-\frac{\partial}{\partial p}\frac{a}{a_0}\simeq\frac{C_{33}-C_{13}}{C_{33}}\frac{1}{C_{11}+C_{12}}\simeq 0.08\frac{C_{33}-C_{13}}{C_{33}}$$

and this indicates that C_{13} has to be negative and of the same order of magnitude as C_{33} in order to explain the behavior of a with pressure. Therefore, the puzzle is why the directly measured value of C_{13} is different from the value derived from the pressure dependence of a. If we can solve this problem we might then be able to understand why our theoretical value is exactly in between the "experimental" numbers.

The samples from which the elastic constants were obtained[17] are compression-annealed pyrolytic graphite (CAPG), while the lattice constants under pressure[16] were measured for natural Ceylon graphite. Compressibility results for CAPG are in reasonable agreement with those of single-crystalline natural graphite.[19] Due to the large anisotropy, however, most properties are mainly determined by $C_{11}+C_{12}$ and, to a smaller extent, by C_{33}; C_{13} does not play a significant role. Hence, the similarity between natural graphite and CAPG is only strongly justified for the in-plane elastic properties.

Measuring C_{13} is not easy[19] and the results for C_{13} at low temperature are not really accurate.[19] But the data in Table VI, lines 2 and 4, pertain to room temperature, and even in this case the difference in the values of C_{13} is larger by a factor of 8 compared to the combined standard deviation. Hence, an experimental error due to the extrapolation to 0 K is not likely to be the cause of the discrepancy.

The negative value of C_{13} indicates that there is a complicated response of the system to uniaxial stress, which is reflected in the charge transfer between π and σ bonds. It is immediately clear that impurities between the carbon layers will have large effects on this mechanism, and it is known that graphite intercalates easily. Also, the effect of dislocations has to be taken into account. Hence different samples might give different results, especially for C_{13} (but hardly for C_{11} and C_{12}). Experiments determining C_{13} on samples with varying, but controlled, amounts of intercalants should reveal the value of C_{13} in the zero impurity limit.

VIII. CONCLUSION

We have performed a highly precise calculation of the total energy of graphite as a function of the lattice constants, preserving the D_{6h}^4 symmetry. The agreement of the calculated lattice constants with experiment is very good, and shows that the local-density approximation does not lead to larger than usual discrepancies for a system like graphite, where the electron density of the valence electrons varies strongly. A comparison of our results with the data of YC (Ref. 5) shows that the effect of the pseudopotential approximation is very small in a system like graphite. A major difference with experiment is obtained for the elastic constant C_{13}, but in this case the experimental results are also contradictory. Clearly, the mechanism connecting the strong covalent in-plane bonds and the weakly covalent interplanar bonds is very sensitive to the presence of impurities between the graphitic layers and dislocations of the layers. Hence there is a need for experiments determining C_{13} in samples with well-controlled defect and impurity concentrations. Only when these results are available will a comparison with our theoretical values be able to assess the effects of the local-density approximation on the theoretical description of this sensitive quantity.

ACKNOWLEDGMENTS

We thank M. Weinert, E. Wimmer, M. Posternak, A. Baldereschi, and I. Spain for helpful discussions. This work was supported by the National Science Foundation (DMR Grant No. 85-18607) and by a computing grant from its Office for Advanced Scientific Computing.

APPENDIX A: NUMERICAL DETAILS

As discussed in our paper describing the bulk FLAPW method,[6] most numerical parameters can be taken large enough to have no significant effects on the total energy while keeping a reasonable computation time. The upper bound of our energy window was taken rather high, because nonspherical terms are large. It was located about 2.5 Ry above the Fermi level, giving rise to about 30 unoccupied states at each **k** point (versus 8 occupied levels). Also the number of plane waves describing the interstitial density and potential was chosen large in order to have enough flexibility in our choice of basis size. We incorporated all plane waves inside a sphere whose radius, multiplied by the muffin-tin sphere radius, was equal to 13.

The two important parameters, which had to be monitored carefully, are (as usual) the number of basis functions and the number of **k**-points inside the irreducible part of the Brillouin zone. All our final calculations were performed with basis functions inside a sphere of half the radius of the sphere described in the previous paragraph, yielding between 500 and 600 basis functions for each **k** point. Even in this case, the total energy still had an absolute error of 10 mRy as compared to its converged value, but the relative error (for different values of a and c) was less than 1 mRy.

The largest relative error was due to the **k** mesh used in the Brillouin-zone integrations. We performed our final

TABLE VII. Total energy differences (in mRy) as a function of the lattice constants a and c (in a.u.). These results are obtained in our final iterations.

a	c	E
4.600	12.654	−0.5
4.600	12.654	−0.7
4.680	12.100	0.8
4.641	12.654	0.0
4.800	12.654	25.9
4.550	12.654	7.9
4.680	12.400	0.2
4.750	11.400	15.1
4.550	11.400	12.7
4.750	13.900	12.2
4.550	13.900	13.6
4.650	13.900	−0.1
4.650	11.400	8.1

iterations with 140 points inside the irreducible wedge of the Brillouin zone, and in this case the absolute error in the total energy was about 5 mRy, as compared to its fully converged value. The relative error, however, was less than 1 mRy, but was responsible for most of our numerical inaccuracies, as presented in our error bars. Since it is also comparable to the size of the anharmonic terms (see Appendix B), it prevented us from determining the exact values of the higher-order terms in the total energy.

Finally, Table VII summarizes our total energy results, given relative to the value at the experimental lattice constants. These results all pertain to the same numerical precision, with 140 points in the irreducible wedge of the Brillouin zone and a large basis.

APPENDIX B: INTERPOLATION OF THE ENTHALPY

We first discuss the second-order expansion of the enthalpy $H=E+pV$. Since we will expand this quantity in terms of the relative deviations from the equilibrium values of the lattice constants at zero pressure, a_0 and c_0, we define

$$\frac{\Delta}{2}=\frac{a-a_0}{a_0}\ , \tag{B1}$$

$$\delta=\frac{c-c_0}{c_0}\ , \tag{B2}$$

with the inverse

$$a=a_0\left[1+\frac{\Delta}{2}\right]\ , \tag{B3}$$

$$c=c_0(1+\delta)\ . \tag{B4}$$

This leads to the following expression for the enthalpy H:

$$H=E_0+pV_0+pV_0(\Delta+\delta)+\left[\alpha+\frac{pV_0}{4}\right]\Delta^2 +(\beta+pV_0)\Delta\delta+\gamma\delta^2\ , \tag{B5}$$

in which we define

$$V_0=\frac{\sqrt{3}}{2}a_0^2c_0\ . \tag{B6}$$

The constants α, β, and γ are directly related to the elastic constants at zero pressure,

$$\alpha=\frac{V_0}{4}(C_{11}+C_{12})\ , \tag{B7}$$

$$\beta=V_0C_{13}\ , \tag{B8}$$

$$\gamma=\frac{V_0}{2}C_{33}\ . \tag{B9}$$

Formula (B5) does not give the derivatives of the elastic constants with pressure: for that case higher-order terms have to be included. The values of the lattice constants at nonzero pressure are found by minimizing (B5) with respect to Δ and δ, which leads to the equations

$$0=\frac{\partial H}{\partial\Delta}=pV_0+2\left[\alpha+\frac{pV_0}{4}\right]\Delta+(\beta+pV_0)\delta\ , \tag{B10}$$

$$0=\frac{\partial H}{\partial\delta}=pV_0+(\beta+pV_0)\Delta+2\gamma\delta\ . \tag{B11}$$

These have the following solution:

$$\Delta=\frac{pV_0}{W}(2\gamma-\beta-pV_0)\ , \tag{B12}$$

$$\delta=\frac{pV_0}{W}(2\alpha-\beta-\tfrac{1}{2}pV_0)\ , \tag{B13}$$

$$W=(\beta+pV_0)^2-4\gamma\left[\alpha+\frac{pV_0}{4}\right]\ , \tag{B14}$$

from which we find immediately

$$\frac{1}{V_0}\frac{\partial\Delta}{\partial p}\bigg|_{p=0}=(2\gamma-\beta)/(\beta^2-4\alpha\gamma)\ , \tag{B15}$$

$$\frac{1}{V_0}\frac{\partial\delta}{\partial p}\bigg|_{p=0}=(2\alpha-\beta)/(\beta^2-4\alpha\gamma)\ , \tag{B16}$$

or in terms of the lattice constants and elastic constants,

$$2\frac{\partial}{\partial p}\frac{a}{a_0}\bigg|_{p=0}=(C_{33}-C_{13})/[C_{13}^2-\tfrac{1}{2}C_{33}(C_{11}+C_{12})]\ , \tag{B17}$$

$$\frac{\partial}{\partial p}\frac{c}{c_0}\bigg|_{p=0}=\left[\frac{C_{11}+C_{12}}{2}-C_{13}\right]\Big/[C_{13}^2-\tfrac{1}{2}C_{33}(C_{11}+C_{12})]\ . \tag{B18}$$

The bulk modulus at zero pressure follows from $B=-V(\partial p/\partial V)$ and is related to the elastic constants by

$$B=\frac{(C_{11}+C_{12})C_{33}-2C_{13}^2}{C_{11}+C_{12}+2C_{33}-4C_{13}} . \tag{B19}$$

The isotropic bulk modulus is obtained by forcing $\Delta/2=\delta$ and we find

$$B_{\rm iso}=\tfrac{2}{9}(C_{11}+C_{12})+\tfrac{4}{9}C_{13}+\tfrac{1}{9}C_{33} . \tag{B20}$$

Higher-order elastic constants do not enter into formulas (B17)—(B20) for the zero pressure derivatives.

In order to discuss the effects of third-order terms we transform to new variables according to

$$x=\Delta/\Delta_R , \tag{B21}$$

$$y=\delta/\delta_R , \tag{B22}$$

where Δ_R and δ_R are the ranges of Δ and δ. Hence x and y are within $[-1,1]$ and the third-order term can now be expressed in Legendre polynomials according to

$$E^3=\sum_{n=0}^{3} C_n^3 P_n(x)P_{3-n}(y) . \tag{B23}$$

Because of the orthogonality of the Legendre polynomials, adding this term to the fitting function does not change the values of the coefficients of the lower-order functions, when they are also expressed in terms of Legendre polynomials. We now replace c_n^3 by ϵ (an assumption to be examined later) and from our data we find that 4ϵ is at most 1 mRy. The internal energy at zero pressure now becomes

$$E=\alpha\Delta_R^2x^2+\beta\Delta_R\delta_Rxy+\gamma\delta_R^2y^2+\epsilon\sum_n P_n(x)P_{3-n}(y) \tag{B24}$$

with approximately the following values of the parameters:

$$\alpha\Delta_R^2=2\times10^{-3} , \tag{B25}$$

$$\beta\Delta_R\delta_R=-4\times10^{-4} , \tag{B26}$$

$$\gamma\delta_R^2=5\times10^{-3} , \tag{B27}$$

$$\epsilon=2\times10^{-4} . \tag{B28}$$

Expression (B24) has to be minimized with respect to x and y. The minimum occurs for $x\simeq0.1$ and $y\simeq0.04$, resulting in errors of about 0.2% for a and about 0.4% for c. These errors are included in Table II. Because of this shift our values of the elastic constants are also affected and we find an error due to higher-order terms in $C_{11}+C_{12}$ of 8%, in C_{33} of 2%, and in C_{13} of 25%. These errors are included in Table VI.

Another check on the size of ϵ comes from the pressure derivatives of the elastic constants. From (B24) we find

$$\frac{\partial^2E}{\partial x^2}=2\alpha\Delta_R^2+\frac{\epsilon}{2}(30x+6y) , \tag{B29}$$

$$\frac{\partial^2E}{\partial x\partial y}=\beta\Delta_R\delta_R+\frac{\epsilon}{2}(6x+6y) , \tag{B30}$$

$$\frac{\partial^2E}{\partial y^2}=2\gamma\delta_R^2+\frac{\epsilon}{2}(30y+6x) , \tag{B31}$$

which translates into

$$\frac{1}{C_{11}+C_{12}}\frac{\partial}{\partial p}(C_{11}+C_{12})=\frac{\epsilon}{4\alpha\Delta_R^2}\frac{\partial}{\partial p}(30x+6y) , \tag{B32}$$

$$\frac{1}{C_{13}}\frac{\partial}{\partial p}C_{13}=-\frac{\epsilon}{2\beta\Delta_R\delta_R}\frac{\partial}{\partial p}(6x+6y) , \tag{B33}$$

$$\frac{1}{C_{33}}\frac{\partial}{\partial p}C_{33}=\frac{\epsilon}{4\gamma\delta_R^2}\frac{\partial}{\partial p}(6x+30y) . \tag{B34}$$

From our data we find for the order of magnitude of these deviations 8, 38, and 6 $\rm Mbar^{-1}$, while the experimental numbers[19] are 4, 21, and 27 $\rm Mbar^{-1}$. This indicates that the order of magnitude of ϵ is correct, but that not all coefficients C_n^3 have the same value of ϵ as was assumed in the derivation of (B24), etc.

[1]We will only compare our results with the most accurate recent work in Refs. 2 and 3; many references to older publications can be found in these two papers.

[2]R. C. Tatar and S. Rabii, Phys. Rev. B **25**, 4126 (1982).

[3]N. A. W. Holzwarth, S. G. Louie, and S. Rabii, Phys. Rev. B **26**, 5382 (1982).

[4]D. P. DiVincenzo, E. J. Mele, and N. A. W. Holzwarth, Phys. Rev. B **27**, 2458 (1983).

[5]M. T. Yin and M. L. Cohen, Phys. Rev. B **29**, 6996 (1984).

[6]H. J. F. Jansen and A. J. Freeman, Phys. Rev. B **30**, 561 (1984).

[7]M. Weinert, E. Wimmer, and A. J. Freeman, Phys. Rev. B **26**, 4571 (1982).

[8]M. Posternak, A. Baldereschi, A. J. Freeman, E. Wimmer, and M. Weinert, Phys. Rev. Lett. **50**, 761 (1983).

[9]W. Eberhardt, J. T. McGovern, E. W. Plummer, and J. E. Fischer, Phys. Rev. Lett. **44**, 200 (1980).

[10]A. Bianconi, S. B. M. Hagström, and R. Z. Bachrach, Phys. Rev. B **16**, 5543 (1977).

[11]A. R. Law, J. J. Barry, and H. P. Hughes, Phys. Rev. B **28**, 5332 (1983).

[12]C. L. Fu, S. Ohnishi, H. J. F. Jansen, and A. J. Freeman, Phys. Rev. B **31**, 1168 (1985).

[13]M. Weinert (private communication).

[14]B. T. Kelly, *Physics of Graphite* (Applied Science, London, 1981), p. 80.

[15]D. Sands, *Introduction to Crystallography* (Benjamin-Cummings, Reading, 1969).

[16]R. W. Lynch and H. Drickamer, J. Chem. Phys. **44**, 181 (1966).

[17]Von A. Ludsteck, Acta Cryst. A **28**, 59 (1972).

[18]O. L. Blackslee, D. G. Proctor, E. J. Seldin, G. B. Spence, and T. Weng, J. Appl. Phys. **41**, 3373 (1970).

[19]W. B. Gauster and J. J. Fritz, J. Appl. Phys. **45**, 3309 (1974).

[20]Reference 14, p. 214.